CALCULATION OF STRESS INTENSITY FACTORS FOR COMBINED MODE BEND SPECIMENS

WANG KEREN (王克仁), XU JILIN (徐纪林),
AND GAO HUA (高 桦)
(*Institute of Mechanics, Academia Sinica*)

Received June 29, 1977.

ABSTRACT

Three methods are used in the calculation of stress intensity factors K_I and K_{II} of combined mode bend specimens, i.e., the boundary collocation method, the finite element method and an approximate method. In the finite element method, special elements are used in a wider area, not restricted in the vicinity of the crack tip. The approximate method employs an approximate relation between K_I and K_{II}, which is introduced in this paper. The results of calculations by different methods are compared with each other and are found in good agreement.

I. INTRODUCTION

In order to test the combined mode fracture criteria experimentally it is necessary to use specimens with a wide range of K_I and K_{II} and to obtain the calibrated curves of K_I and K_{II} values for these specimens either by calculation or by experiment. As no such calculated curves of K_I and K_{II} values are readily available for three-point-bend specimens with cracks in an unsymmetrical position (Fig. 1), such curves are obtained by use of the boundary collocation method and the finite element method. The boundary

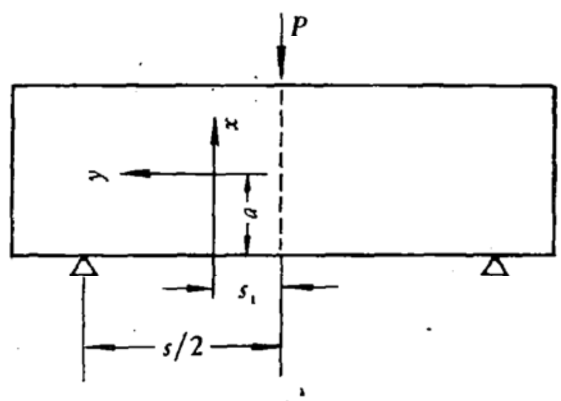

Fig. 1. Three-point-bend specimen with crack in unsymmetrical position.

collocation method was first used by Gross *et al.*[1-3] to calculate K_I values for opening mode specimens. Later the method was used to calculate K_I and K_{II} values for some combined mode specimens[4,5]. As for the finite element method used to determine stress intensity factors, a growing interest is now directed to the special elements at the crack tip[6,7]. A term of $\sqrt{r}$ is included in the displacement functions of these special elements, where r is the distance of the given point to the crack tip. As this term gives the required singularities of stresses and strains in the vicinity of the crack tip, a higher accuracy can often be obtained with relatively fewer elements. Since the other elements around the special elements are still ordinary ones, whose displacement functions do not contain the terms of $\sqrt{r}$, the results obtained by the use of these special elements are, therefore, not very satisfactory, especially in the case when the size of the elements is getting smaller. It should be noted that the convergence of the results cannot be ensured for the elements of diminishing size, if the condition of constant strain is not satisfied by those special elements[8], as is the case with the commonly adopted ones. However, the distorted isoparametric elements, proposed by Henshell *et al.*[9] and Barsoum[10], satisfy the constant strain condition and their displacement functions contain the terms of $\sqrt{r}$. The 8-noded isoparametric quadratic and triangular elements with the mid-side nodes near the crack tip at the quarter point have been used in the vicinity of the crack tip and their displacement functions contain the terms of $\sqrt{r}$. Now we have succeeded in including the terms of $\sqrt{r}$ in the displacement functions of any isoparametric elements at any arbitrary positions. When these special elements are used in a wider area, not restricted in the vicinity of the crack tip, the accuracy of the calculated results is improved considerably.

On analysing the energy-momentum tensor, which was proposed by Eshelby[11] and was later used in the combined mode fracture criteria by Hellen *et al.*[12], it was pointed out that this kind of application of the energy-momentum tensor is questionable theoretically, and that the results thus obtained are doubtful[13]. In the meantime, an approximate relation between K_I and K_{II} is used to derive the approximate formula of K_{II} for the bend specimens mentioned above. The results calculated by this formula are compared with that of the boundary collocation method.

II. Boundary Collocation Method

Consider the following expansion of the stress function with the crack tip as the centre:

$$\chi = \sum_{j=1}^{\infty} r^{\frac{j}{2}+1} \left\{ C_j \left[-\cos\left(\frac{j}{2}-1\right)\theta + \frac{\frac{j}{2}+(-1)^j}{\frac{j}{2}+1}\cos\left(\frac{j}{2}+1\right)\theta \right] \right.$$

$$\left. + D_j(-1)^{j+1}\left[\sin\left(\frac{j}{2}-1\right)\theta - \frac{\frac{j}{2}+(-1)^{j+1}}{\frac{j}{2}+1}\sin\left(\frac{j}{2}+1\right)\theta \right] \right\}. \quad (1)$$

According to the approach adopted by Gross *et al.*[1,2,3], the expansion is truncated to the first $2N$ terms and M ($M \geqslant N$) points on the boundary of the specimen are chosen. From the boundary conditions on these M points, $2M$ equations are obtained and the $2N$ coefficients in the truncated expansion can be determined. The values of K_I and K_{II} are determined from the first two coefficients:

$$K_I = -C_1\sqrt{2\pi}, \qquad K_{II} = D_1\sqrt{2\pi}. \tag{2}$$

Note that as the term of D_2 in Eq. (1) is identical with zero, this term should be deleted from the resulting simultaneous equations, otherwise an overflow will take place during the calculation if M is equal to N. The overflow was mentioned in [4] by Wilson *et al.*, and the reason is now explained here.

We take 43 terms and choose 63 collocation points. The calculated results are shown in Table 1. It can be seen from Table 1 that $K_IBW^{3/2}/M$ and $K_{II}BW^{1/2}/Q$ depend only on a/W in a wide range (so far as the crack tip is not very close to the concentrated forces and the support points). It follows that the values of K_I and K_{II} can be determined approximately by the bending moment and the shearing force on the crack section, respectively.

Table 1

Calculated Results of K_I^* and K_{II}^* for Three-Point-Bend Specimens With $s/W=4$ by Boundary Collocation Method

a/W \ $2s_1/s$		0	1/6	2/6	3/6	4/6	5/6	11/12
0.40	K_I^*	7.71	8.50	8.55	8.36	8.33	8.50	8.50
	K_{II}^*	0	1.032	1.400	1.350	1.298	1.376	1.644
0.45	K_I^*	8.86	9.67	9.72	9.38	9.48	9.55	
	K_{II}^*	0	1.142	1.562	1.488	1.466	1.464	
0.50	K_I^*	10.27	11.48	11.50	11.60	11.15	11.59	11.53
	K_{II}^*	0	1.410	1.864	1.840	1.664	1.660	1.760
0.55	K_I^*	12.11	13.30	13.60	13.03	12.90	13.46	
	K_{II}^*	0	1.588	1.980	2.050	1.976	2.100	
0.60	K_I^*	14.47	14.25	14.65	14.91	14.88	14.74	14.50
	K_{II}^*	0	2.348	2.248	2.276	2.320	2.294	2.090

$K_I^* = K_IBW^{3/2}/M \qquad K_{II}^* = K_{II}BW^{1/2}/Q$

III. Finite Element Method

An 8-noded isoparametric quadratic element is shown in Fig. 2. Its shape functions are

$$N_i = \frac{1}{4}(1+\xi_i\xi)(1+\eta_i\eta)(\xi_i\xi+\eta_i\eta-1)$$

for the corner nodes,

$$N_i = \frac{1}{2}(1-\xi^2)(1+\eta_i\eta) \tag{3}$$

for the mid-side nodes with $\xi_i = 0$, and

$$N_i = \frac{1}{2}(1+\xi_i\xi)(1-\eta^2)$$

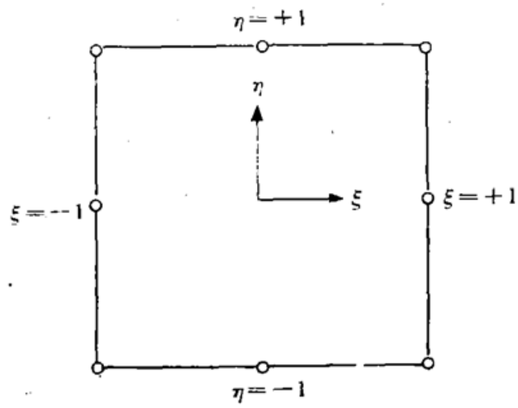

Fig. 2. 8-noded isoparametric quadratic element.

for the mid-side nodes with $\eta_i = 0$. Taking the side $\eta = +1$, we have (Fig. 3)

$$N_1 = -\frac{\xi(1-\xi)}{2},$$
$$N_2 = 1 - \xi^2, \tag{4}$$
$$N_3 = \frac{\xi(1+\xi)}{2}.$$

By the coordinate transformation used for the isoparametric elements, this side is assumed to be mapped into a segment AB on a line passing through the crack tip O (Fig. 3).

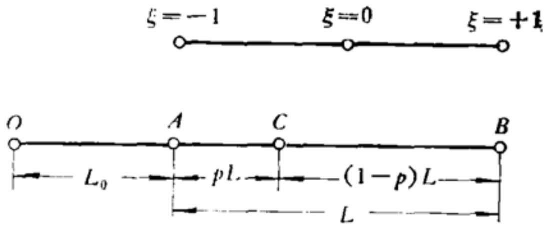

Fig. 3. Distorted side of 8-noded isoparametric element.

The lengths of OA and AB are equal to L_0 and L, respectively. The point, $\xi = 0$, is mapped into a point C, which is supposed to divide the segment AB into a ratio of p and $(1-p)$. If the coordinate on the segment AB, after the transformation, is denoted by x, it follows that

$$x = -\frac{\xi(1-\xi)}{2} L_0 + (1-\xi^2)(L_0 + pL) + \frac{\xi(1+\xi)}{2}(L_0 + L). \tag{5}$$

Let $L_0/L = k$, it can be shown that

$$\xi = -[1 + 2k + \sqrt{4k(k+1)}] + 2(\sqrt{1+k} + \sqrt{k})\sqrt{\frac{x}{L}}, \tag{6}$$

when

$$p = \frac{1}{4}[\sqrt{4k(k+1)} + 1 - 2k]. \tag{7}$$

By substituting Eq. (6) into the relevant formulas of the isoparametric element, we obtain the expressions for the displacement that include the terms of $\sqrt{r}$. Let $k=0$, the relations given in [9] and [10] can be obtained. From Eq. (7), it is easily seen that p approaches 1/2 as k is getting larger. That is to say that the distorted elements approach the normal (undistorted) ones as the elements are getting farther away from the crack tip.

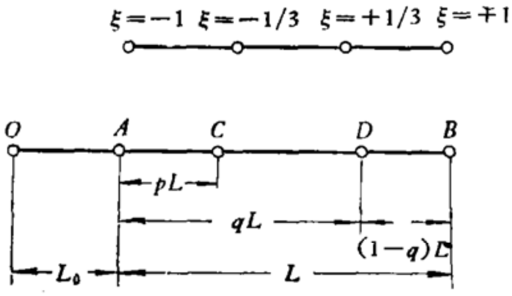

Fig. 4. Distorted side of 12-noded isoparametric element.

For the 12-noded isoparametric quadratic element (see [8]), if we assume that the mid-side nodes of the distorted elements divide the side into a ratio of p, $(q-p)$, and $(1-q)$ (Fig. 4), it can be shown that Eq. (6) is again established, when

$$
\begin{aligned}
p &= \frac{1}{9}\left[1-4k+4\sqrt{k(k+1)}\right],\\
q &= \frac{1}{9}\left[4-4k+4\sqrt{k(k+1)}\right].
\end{aligned}
\tag{8}
$$

The corresponding expressions for the displacement thus obtained contain the terms of $\sqrt{r}$ and $r\sqrt{r}$.

To test the method we consider the three-point-bend specimen with the crack at a symmetrical position. The geometry of the specimen and its finite element idealization are shown in Fig. 5. In the vicinity of the crack tip we use triangular elements, which were shown to be superior to the quadratic ones[10].

First we use the same procedure as given in [10]. Only those triangular elements in the vicinity of the crack tip are taken to be distorted ones, with the mid-side nodes near the crack tip at the quarter point and all other elements taken to be normal ones. The final results are shown in Fig. 6a. By the use of the calculated values of the displacements of the points on the crack edges, the apparent values of the stress intensity factors can be determined by

$$
\bar{K}_I = \frac{E}{4(1-\nu^2)}\sqrt{\frac{2\pi}{r}}\,u, \tag{9}
$$

where $\bar{K}_I$ is plotted against the distance r. By analysing the expansion of the displacement at the crack tip, it can be shown that the apparent value $\bar{K}_I$ is a linear function of r, if r is sufficiently small. The intersecting point of the straight part of the curve on the vertical axis $(r=0)$ gives the true K_I value. Some points near the crack tip

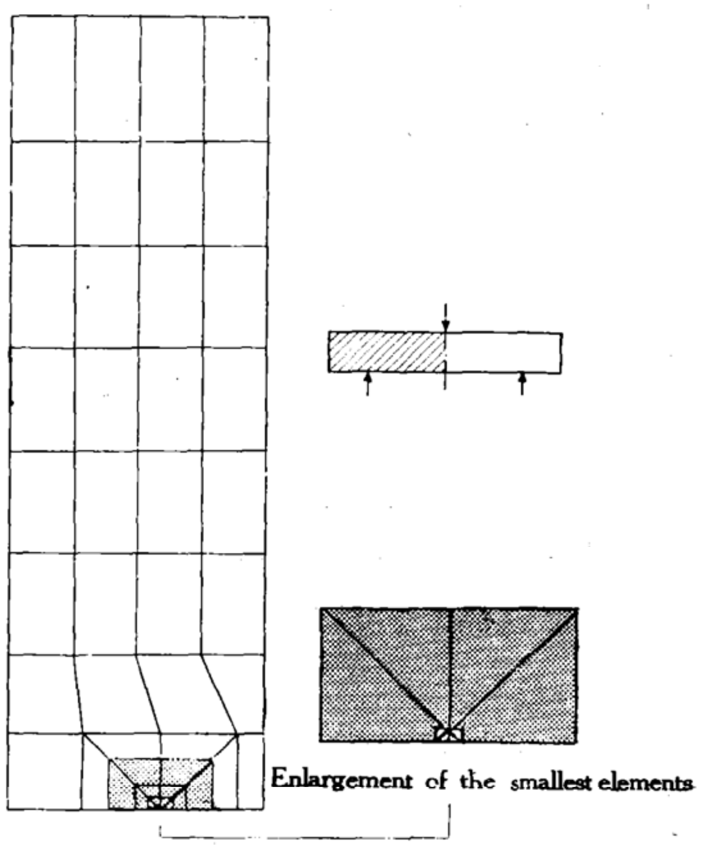

Fig. 5. Finite element idealization of three-point-bend specimen with crack in symmetrical position, $a/W = 0.4$.

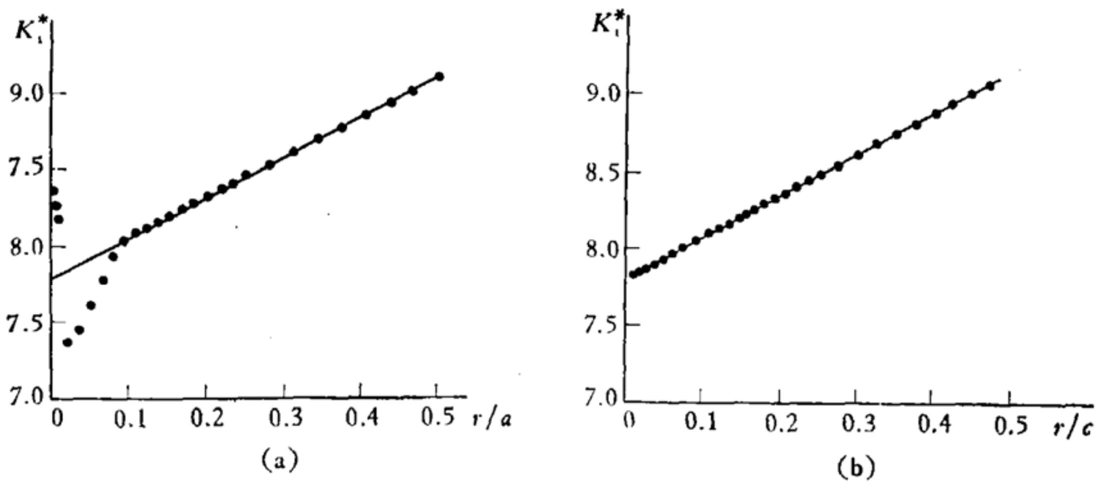

Fig. 6. Apparent values of stress intensity factors for specimen shown in Fig. 5.
(a) Special elements are restricted in the vicinity of crack tip;
(b) Special elements are not restricted in the vicinity of crack tip.

that deviates from the straight line can be seen in Fig. 6a. This indicates that these apparent values of K_I are questionable and should be discarded.

Secondly, we re-calculate the mid-side nodes according to Eq. (7) for all elements in the shaded area of Fig. 5. The final results are shown in Fig. 6b. The curve is superior to that of Fig. 6a in the sense that all points near the crack tip fall on a straight line, as expected from the analysis. The intersecting point gives $K_I B W^{3/2}/M = 7.79$, with $a/W = 0.4$. It is in good agreement with the result calculated by the boundary collocation method: $K_I B W^{3/2}/M = 7.71$.

IV. Approximate Relation Between K_I and K_{II}

For any plane configuration with a crack as shown in Fig. 7, it can be proved that

$$J_1 = -\frac{\partial U}{\partial l} = \int_C W dy - \mathbf{T} \cdot \frac{\partial \mathbf{u}}{\partial x} ds, \tag{10}$$

$$J_2 = -\frac{\partial U}{\partial s} = \int_C - W dx - \mathbf{T} \cdot \frac{\partial \mathbf{u}}{\partial y} ds, \tag{11}$$

where U is the total potential energy of the system and C is the exterior contour of the configuration. Eq. (11) gives the rate of the increase of the total potential energy

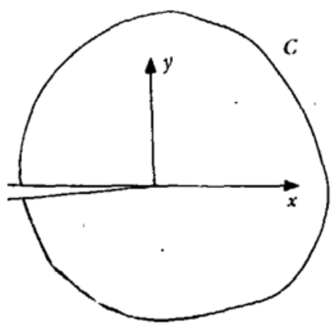

Fig. 7. Plane configuration with crack.

as the crack translates in the direction perpendicular to the crack. Eq. (10) defines the J-integral, whose value is path-independent, so long as the path starts at the lower edge of the crack and ends at the upper edge. As for Eq. (11), it can be proved that the value of the integral is also path-independent, if the points on the crack edges remain intact[11]. If a contour D sufficiently near the crack tip is taken, it can be shown that

$$\begin{aligned} J_1' &= \int_D W dy - \mathbf{T} \cdot \frac{\partial \mathbf{u}}{\partial x} ds = \frac{(1+\nu)(1+\kappa)}{4E} (K_I^2 + K_{II}^2), \\ J_2' &= \int_D - W dx - \mathbf{T} \cdot \frac{\partial \mathbf{u}}{\partial y} ds = -\frac{(1+\nu)(1+\kappa)}{4E} \cdot 2K_I K_{II}, \end{aligned} \tag{12}$$

where

$$\kappa = \begin{cases} \dfrac{3-\nu}{1+\nu}, & \text{for plane stress.} \\ 3-4\nu, & \text{for plane strain,} \end{cases} \tag{13}$$

Due to the properties of J-integral, J_1 is equal to J_1'. It can be shown that

$$R = J_2' - J_2 = \int_{\Gamma_1+\Gamma_2} W dx = \frac{(1+\nu)(1+\kappa)}{8E} \int_{\Gamma_1+\Gamma_2} \sigma_x^2 dx, \tag{14}$$

where Γ_1 and Γ_2 are the upper and lower edges of the crack respectively. For the upper edge the integration proceeds from left to right and for the lower edge from right to left. Since σ_x^2 takes the same value on the upper and lower edges in the vicinity of the crack tip and σ_x dwindles when the point moves towards the open end of the crack, it is expected that R will be a small quantity and will not be very sensitive to a small change in the crack length. So it is reasonable to assume that

$$\frac{\partial R}{\partial l} \approx 0. \tag{15}$$

Combining Eqs. (15), (10), (11), and (12), we obtain

$$\frac{\partial J_1'}{\partial s} \approx \frac{\partial J_2'}{\partial l}, \tag{16}$$

from which we obtain the following approximate relation between K_I and K_{II}:

$$K_{II} \frac{\partial K_I}{\partial l} + K_I \frac{\partial K_{II}}{\partial l} + K_I \frac{\partial K_I}{\partial s} + K_{II} \frac{\partial K_{II}}{\partial s} = 0. \tag{17}$$

If we further assume that K_I and K_{II} can be determined by the bending moment M and the shearing force Q on the crack section respectively, we can write

$$\begin{aligned} K_I &= \frac{M}{BW^{\frac{3}{2}}} f_b\left(\frac{a}{W}\right), \\ K_{II} &= \frac{Q}{BW^{\frac{1}{2}}} f_s\left(\frac{a}{W}\right). \end{aligned} \tag{18}$$

After substituting Eq. (18) into Eq. (17), we get the following equation:

$$f_b\left(\frac{a}{W}\right) \frac{df_s\left(\frac{a}{W}\right)}{d\left(\frac{a}{W}\right)} + \frac{df_b\left(\frac{a}{W}\right)}{d\left(\frac{a}{W}\right)} f_s\left(\frac{a}{W}\right) - \left[f_b\left(\frac{a}{W}\right)\right]^2 = 0. \tag{19}$$

The equation is solved to obtain

$$f_s\left(\frac{a}{W}\right) = \frac{1}{f_b\left(\frac{a}{W}\right)} \int_0^{a/W} \left[f_b\left(\frac{a}{W}\right)\right]^2 d\left(\frac{a}{W}\right). \tag{20}$$

For $f_b(a/W)$, we make use of the results for pure bending due to Benthem et al.[14]. The calculated values of $f_s(a/W)$ according to Eq. (20) are given in Table 2 and are in reasonably good agreement with the results calculated by the boundary collocation method.

Table 2

Calculated Results by Eq. (20)

a/W	$f_b(a/W)$	$f_s(a/W)$	$f'_s(a/W)$	Difference in Percentage
0.05	2.54	0.0636		
0.10	3.51	0.180		
0.15	4.26	0.327		
0.20	4.97	0.496		
0.25	5.67	0.667		
0.30	6.45	0.857		
0.35	7.32	1.080		
0.40	8.35	1.317	1.350	−2.5
0.45	9.60	1.557	1.488	4.4
0.50	11.12	1.838	1.840	−0.1
0.55	13.09	2.125	2.050	3.5
0.60	15.66	2.441	2.276	6.8
0.65	19.17	2.794		
0.70	24.15	3.077		

Note: $f_b(a/W)$ and $f_s(a/W)$ are identical with K_I^* and K_{II}^* in Table 1. $f'_s(a/W)$ is calculated by the boundary collocation method for the case $2s_1/s = 3/6$.

V. Concluding Remarks

This paper has outlined the results of three methods used in the calculation of K_I and K_{II} of the combined mode bend specimens. If an estimate is to be made at the design stage of an experiment, the results (Table 2) calculated from the approximate relation of Section 4 can be used. K_I and K_{II} can be determined by the crack length a/W, the bending moment and the shearing force on the crack section. The final calculation for a specimen may be made by the boundary collocation method or the finite element method.

References

[1] Gross, B., Srawley, J. E., & Brown, Jr. W. F.: Stress-intensity factors for a single-edge-notch tension specimen by boundary collocation of a stress function, *NASA TN D*-2395, 1964.

[2] Gross, B. & Srawley, J. E.: Stress-intensity factors for a single-edge-notch specimens in bending or combined bending and tension by boundary collocation of a stress function, *NASA TN D*-2603, 1965.

[3] Gross, B. & Srawley, J. E.: Stress-intensity factors for three-point-bend specimens by boundary collocation, *NASA TN D*-3092, 1965.

[4] Wilson, W. K., Clark, W. G., & Wessel, E. T.: Fracture mechanics technology for combined loading low to intermediate strength metals, *AD*-682754, 1968.

[5] Wilson, W. K.: Numerical method for determining stress intensity factors of an interior crack in a finite plate, *Trans. ASME Series D*, **93** (1971), 685.

[6] Hilton, P. D. & Sih, G. C.: Application of the finite element method to the calculation of stress intensity factors, *Methods of Analysis and Solutions of Crack Problems*, (ed. Sih, G. C.), (1972), Noordhoff International Publishing.

[7] Wilson, W. K.: Finite element metheds for elastic bodies containing cracks, *Methods of Analysis and Solutions of Crack Problems*, (ed. Sih, G. C.), (1972), Noordhoff International Publishing.
[8] Zienkiewicz, O. C.: *The Finite Element Method in Engineering Science*, (1971), McGraw-Hill Publishing Company Limited.
[9] Henshell, R. D. & Shaw, K. G.: Crack tip finite elements are unnecessary, *Int. J. Numerical Method in Engineering*, **9** (1975), No. 3, 495.
[10] Barsoum R. S.: On the use of isoparametric finite elements in linear fracture mechanics, *Int. J. Numerical Method in Engineering*, **10** (1976), No. 1, 25.
[11] Eshelby, J. R.: The continuum theory of lattice defects, *Solid State Physics*, Vol. 3, (1956).
[12] Hellen, T. K. *et al.*: The calculation of stress intensity factors for combined tensile and shear loading, *Int. J. Fracture*, **11** (1975), 605.
[13] Energy-momentum tensor and its application in fracture mechanics (in Chinese), Research Paper of Institute of Mechanics, Academia Sinica, 1976.
[14] Benthem, J. P. & Koiter, W. T.: Asymptotic approximations to crack problems, *Methods of Analysis and Solutions of Crack Problems*, (ed. Sih, G. C.), (1972), Noordhoff International Publishing.